Journal of Clinical and Translational Hepatology **2024** vol. 12(2) | 134–150
DOI: 10.14218/JCTH.2023.00171

Original Article

ADAR1 Inhibits Macrophage Apoptosis and Alleviates Sepsis-induced Liver Injury Through miR-122/BCL2A1 Signaling

Shanshou Liu[1#], Jiangang Xie[1#], Chujun Duan[1], Xiaojun Zhao[1], Zhusheng Feng[1], Zheng Dai[1], Xu Luo[1], Yu Li[2], Minghe Yang[3], Ran Zhuang[4], Junjie Li[1*] and Wen Yin[1*]

[1]Emergency Department, Xijing Hospital, Fourth Military Medical University, Xi'an, Shaanxi, China; [2]Emergency Department, Tangdu Hospital, Fourth Military Medical University, Xi'an, Shaanxi, China; [3]Third Student Brigade, School of Basic Medical Science, Fourth Military Medical University, Xi'an, Shaanxi, China; [4]Department of Immunology, Fourth Military Medical University, Xi'an, Shaanxi, China

Received: 14 April 2023 | **Revised:** 18 August 2023 | **Accepted:** 9 October 2023 | **Published online:** 13 November 2023

Abstract

Background and Aims: As sepsis progresses, immune cell apoptosis plays regulatory roles in the pathogenesis of immunosuppression and organ failure. We previously reported that adenosine deaminases acting on RNA-1 (ADAR1) reduced intestinal and splenic inflammatory damage during sepsis. However, the roles and mechanism of ADAR1 in sepsis-induced liver injury remain unclear. ***Methods:*** We performed transcriptome and single-cell RNA sequencing of peripheral blood mononuclear cells (PBMCs) from patients with sepsis to investigate the effects of ADAR1 on immune cell activities. We also employed a cecal ligation and puncture (CLP) sepsis mouse model to evaluate the roles of ADAR1 in sepsis-induced liver injury. Finally, we treated murine RAW 264.7 macrophages with lipopolysaccharide to explore the underlying ADAR1-mediated mechanisms in sepsis. ***Results:*** PBMCs from patients with sepsis had obvious apoptotic morphological features. Single-cell RNA sequencing indicated that apoptosis-related pathways were enriched in monocytes, with significantly elevated ADAR1 and BCL2A1 expression in severe sepsis. CLP-induced septic mice had aggravated liver injury and Kupffer cell apoptosis that were largely alleviated by ADAR1 overexpression. ADAR1 directly bound to pre-miR-122 to modulate miR-122 biosynthesis. miR-122 was an upstream regulator of BCL2A1. Furthermore, ADAR1 also reduced macrophage apoptosis in mice with CLP-induced sepsis through the miR-122/BCL2A1 signaling pathway and protected against sepsis-induced liver injury. ***Conclusions:*** The findings show that ADAR1 alleviates macrophage apoptosis and sepsis-induced liver damage through the miR-122/BCL2A1 signaling pathway. The study provides novel insights into the development of therapeutic interventions in sepsis.

Citation of this article: Liu S, Xie J, Duan C, Zhao X, Feng Z, Dai Z, *et al*. ADAR1 Inhibits Macrophage Apoptosis and Alleviates Sepsis-induced Liver Injury Through miR-122/BCL2A1 Signaling. J Clin Transl Hepatol 2024;12(2):134–150. doi: 10.14218/JCTH.2023.00171.

Introduction

Sepsis, which is defined as "life-threatening organ dysfunction caused by a dysregulated host response to infection" is a leading cause of morbidity and mortality in intensive care units worldwide.[1] In 2017, almost 50 million sepsis cases and 11 million sepsis-associated deaths were reported globally.[2] In clinical practice, six major organ systems of patients with sepsis are often damaged and monitored: cardiovascular, respiratory, renal, neurological, hematological, and hepatic systems.[3] Of those, the liver is heavily exposed to circulating antigens, endotoxins, cellular signals, and microorganisms during microbial infection. Sepsis-induced liver injury is a common complication that occurs during early sepsis and may cause sepsis-related inflammatory pathogenesis,[4] multiple organ dysfunction, and high mortality.[5]

The pathogenesis of sepsis is complicated and involves multiple physiological and pathological processes, including inflammatory imbalance, immune dysfunction, mitochondrial damage, and coagulation disorders.[6] Once liver injury occurs, many monocytes and other innate myeloid cells are rapidly recruited to the sites of injury. These cells, together with the liver Kupffer cells, recognize the released foreign antigens and respond to the infection by triggering immune inflammatory responses to eliminate the pathogens.[7] As the first responders and gatekeepers for the clearance of pathogens, Kupffer cells are postulated to have a central role in the hepatic innate immune system,[8,9] by which 70–80% of the bacteria that enter the blood are removed.[10] As sepsis

Keywords: Sepsis; Macrophage; ADAR1; microRNA122; BCL2A1; Apoptosis.
Abbreviations: ADAR1, adenosine deaminases acting on RNA-1; A-to-I, adenosine-to-inosine; CLP, cecal ligation and puncture; DEGs, differentially expressed genes; ELISA, enzyme-linked immunosorbent assay; GO, gene ontology; KEGG, kyoto encyclopedia of genes and genomes; LPS, lipopolysaccharide; miRNAs, microRNAs; mRNA, messenger RNA; PBMCs, peripheral blood mononuclear cells; PCR, polymerase chain reaction.
[#]Contributed equally to this work.
[*]**Correspondence to:** Wen Yin and Junjie Li, Department of Emergency, Xijing Hospital, Fourth Military Medical University, 127 West Changle Road, Xi'an, Shaanxi 710032, China. ORCID: https://orcid.org/0000-0002-8108-1951 (WY), https://orcid.org/000-0002-5805-7646 (JL). Tel: +86-29-84775535 (WY), +86-29-84771786 (JL), E-mail: xjyyyw@126.com (WY), lijunjie@fmmu.edu.cn (JL)

progresses, monocyte and macrophage apoptosis increases, which may cause immunosuppression and a high risk of secondary infection or mortality.[11] Immune cell apoptosis is pivotal during sepsis-induced immunosuppression and seriously impairs host antimicrobial defenses and microorganism clearance, leading to protracted inflammatory responses. Therapeutic intervention using anti-apoptotic strategies, such as modulating the Bcl2 family, helps to improve prognosis and reduce the mortality of patients with sepsis.[12]

Adenosine deaminases acting on RNA-1 (ADAR1) target double-stranded RNA (dsRNA) and have adenosine-to-inosine (A-to-I) RNA editing activity that has been shown to regulate the biosynthesis of protein-coding genes and microRNAs (miRNAs).[13] Studies have revealed that ADAR1 has an important role in maintaining homeostasis.[14] We previously found that ADAR1 alleviated sepsis-induced inflammation and maintained intestinal homeostasis by interfering with miR-30a biogenesis.[15,16] Moreover, ADAR1 regulates macrophage polarization by binding to miR-21 precursors to modulate its biogenesis.[17] Because immune inflammatory responses are causally involved in the pathogenesis and progression of sepsis, the effects of ADAR1 on sepsis-induced immune cell apoptosis and liver damage have attracted our attention. Given the crucial role of macrophage apoptosis in sepsis-induced immunosuppression, we aimed to explore the underlying mechanism by which ADAR1 modulates macrophage apoptosis in sepsis-induced liver injury. We performed transcriptome and single-cell RNA sequencing of PBMCs from patients with sepsis and evaluated their roles through *in vivo* and *in vitro* sepsis models.

Methods

Ethics statement

This study was approved by the Ethical Committee of our Hospital, with document numbers of KY20212172 and NCT05229328. All procedures involving human participants complied with the Declaration of Helsinki. Informed consent was signed by all healthy volunteers and patients with sepsis. Animal experiments were carried out according to the Guide for the Care and Use of Laboratory Animals and approved by the Institutional Animal Care and Use Committee of our University (approved number: 20220930).

Study population and PBMC collection

Between January and March 2022, a total of 86 sepsis patients were admitted to the emergency department and intensive care unit of the Xijing Hospital. Twenty-eight patients at the early stage of sepsis were involved in this study. Ten healthy volunteers were recruited as the control group. The inclusion criteria for the patients with sepsis were sepsis 3.0=infection plus a sequential organ failure assessment (SOFA) score ≥2; time after diagnosis of <6 h; 18–90 years of age; and no history of serious chronic disease. Patients with tumors and immune system diseases were excluded. Patients who had a blood lactic acid concentration >2 mmol/L and needed vasoactive drugs to maintain a mean arterial pressure (MAP) ≥65 mmHg were identified as having septic shock (severe sepsis [S]); the others were considered to have mild sepsis (M). All subjects were managed following recently updated international guidelines.[18] A total of 8 mL of venous blood was taken from the cubital vein of the patients within 6 h of admission. Plasma and PBMC samples were collected and stored at −80°C for further use.

Bulk RNA sequencing

PBMC samples were sent to Gene Denovo Biotechnology Co. (Guangzhou, China) for messenger RNA (mRNA) and miRNA sequencing. For transcriptome sequencing, oligo (dT) beads were used to enrich mRNA that were then broken into short fragments and reverse transcribed into complementary DNA (cDNA). After purification, end repair, and adding a poly (A) tail, cDNA fragments were ligated to Illumina sequencing adapters and sequenced with the Illumina Novaseq 6000 (San Diego, CA, USA). For miRNA sequencing, 18–30 nucleotide strands were enriched with polyacrylamide gel electrophoresis followed by adding 3′ adapters and then enriching the RNA molecules with a length of 36–44 bp. After ligating 5′ adapters to the RNA, amplification was conducted and the polymerase chain reaction (PCR) products 140–160 bp in length were selected to construct the cDNA libraries that were then sequenced with the Illumina Novaseq 6000.

Single-cell RNA sequencing

Single-cell RNA sequencing was performed with a Chromium (10X Genomics, Pleasanton, CA, USA) sequencing instrument (Gene Denovo Biotechnology Co.). The gene expression library was sequenced using an Illumina Novaseq 6000.

Functional analysis of differentially expressed genes (DEGs)

The transcripts or miRNAs with a ≥2-fold change and p-value of <0.05 were regarded as DEGs or differentially expressed miRNAs. The screened DEGs were mapped to Gene Ontology (GO) terms to determine which were significantly enriched. Pathway enrichment analysis was performed using the Kyoto Encyclopedia of Genes and Genomes (KEGG) database.

Enzyme-linked immunosorbent assay (ELISA)

The plasma concentrations of apoptosis-related molecules (BID, BAX, BCL2A1, BCL2, TNFSF10, and NLRP3) were determined with ELISA kits (Jiang Lai Biotechnology Co., Ltd., Shanghai, China) according to the manufacturer's instructions. The plasma concentrations of murine cytokines, interleukin (IL)-6, apoptosis-related molecules (BAX, BCL2A1a), and markers of liver injury (Glutamic pyruvic transaminase, [GPT], alanine transaminase [ALT], glutamic oxaloacetic transaminase [GOT], and aspartate aminotransferase [AST]) were also determined with ELISA kits (Jiang Lai Biotechnology Co., Ltd.).

Luminex assay

Serum cytokine (IL6, tumor necrosis factor alpha [TNF-α], C-C motif chemokine ligand 4 [CCL4], CXC motif chemokine ligand 2 [CXCL2], macrophage inflammatory protein 3 [MIP3], and MIP3β) concentrations in 28 patients with sepsis and six healthy volunteers were determined by Luminex assays using a Human XL Cytokine Luminex Performance Panel Premixed kit (#FCSTM18-30; R&D Systems, Minneapolis, MN, USA) according to the manufacture instructions. The plates were read using Luminex 200 instrument (Austin, TX, USA).

Scanning electron microscopy (SEM) and transmission electron microscopy (TEM)

For SEM, PMBCs and RAW 264.7 cells were fixed with electron microscope fixatives (#CR2202015; Servicebio, Wuhan, China) in the dark for 30 m. Specimens were attached to metallic stubs, sputter-coated with gold for 30 s, observed, and photographed (SU8100; Hitachi Tokyo, Japan). For TEM, cells were pre-embedded in agarose, dehydrated, infiltrated, and embedded in resin, sectioned at 60–80 nm (EM UC7 ultramicrotome; Leica, Wetzlar, Germany) and placed on 150-mesh formvar coated copper grids and staining with uranium

acetate and lead citrate. The samples were observed and photographed (HT7800; Hitachi).

Septic mouse model

Male C57BL/6 mice (20–25 g and 8–10 weeks of age) were obtained from the animal center of the Fourth Military Medical University. They were housed under standard laboratory conditions for 1 week before being used for experiments. The mice were randomly divided into sham, CLP, and CLP + ADAR1 overexpression groups. CLP surgery is a widely used experimental method to establish sepsis in mice and was performed as described previously.[19] Sham mice were treated identically except that the cecum was neither ligated nor punctured. The CLP + ADAR1 overexpressing mice were treated with 1×10^8 plaque-forming units of ADAR1-overexpressing adenovirus (GenePharma, Shanghai, China) dissolved in 200 μL phosphate-buffered saline (PBS) via tail vein injection. Serum, liver, and lung samples were collected for histological analysis at 0 (sham), 6, 24, and 48 h after surgery. Subsequent animal experiments were performed 24 h after CLP administration. Disease severity was determined by an experienced pathologist based on postoperative manifestations of CLP. The pathologist was blind to the treatment. Disease scoring included five aspects, appearance (score 0–4), behavioral changes at rest (score 0–3) and after stimulation (score 0–3), respiratory signs (score 0–3), and corneal secretions (score 0–5).[20]

Cell culture and treatment

RAW 264.7 macrophages were purchased from the Cell Culture Center, Chinese Academy of Medical Sciences (Beijing, China). Macrophages were activated by lipopolysaccharide (LPS) (#L2880, Sigma-aldrich, Germany) to establish an *in vitro* sepsis model as previously described.[21] RAW 264.7 cells were cultured in serum-free Opti-MEM (Gibco, Brooklyn, NY, USA) 1 h before transfection with ADAR1-overexpressing adenovirus (GenePharma), ADRA1-small interfering RNA (siRNA) (RiboBio, Guangzhou, China), an miR-122 mimic, an miR-122 inhibitor (RiboBio), or a negative control using Lipofectamine 3000 transfection reagent (Invitrogen, Waltham, MA, USA) according to the manufacturer's instructions. The cells were treated with LPS for another 24 h after transfection and collected for subsequent experiments 12 h after the LPS treatment ended.

Hematoxylin and eosin (HE) staining

Liver and lung tissues were harvested, fixed, dehydrated, paraffin embedded, sectioned at 5 μm, and stained with HE (Servicebio). The stained sections were observed with an upright light microscope (Nikon Eclipse E100, Tokyo, Japan). Pathological damage to liver and lung tissue in each group was evaluated by an experienced pathologist in five random fields of each slice using previously published scoring criteria with a slight modification. The pathologist was blind to the treatment of each mouse. Liver injury scoring included four criteria described in the Ishak scoring system, the degree of interface hepatitis (score 0–4), confluent necrosis (score 0–6), lobular inflammation (score 0–4), and portal inflammation (score 0–4).[22,23] Lung damage scoring included four criteria, pulmonary interstitial edema (score 0–4), alveolar edema (score 0–4), inflammatory infiltration (score 0–4), and alveolar hemorrhage (score 0–4).[24] The final score was obtained by summing the individual scores.

Immunohistochemical (IHC) staining

Paraffin-embedded liver tissue was dewaxed and rehydrated followed by antigen retrieval in a citrate solution (pH 6.0) (Servicebio). After blocking to prevent nonspecific protein binding, the sections were incubated with an anti-ADAR1 primary antibody (#SC-73408; Santa Cruz Biotechnology, Dallas, TX, USA) in a wet box at 4°C overnight. The sections were then incubated with horseradish peroxidase-conjugated secondary antibody. A diaminobenzidine (DAB) chromogenic kit (#G1212; Servicebio) was used for visualization. Hematoxylin was used to counterstain nuclei. The sections were observed with research slide scanner (#VS200; Olympus, Tokyo, Japan) after mounting. The mean number of positively stained cells and the density of the chromogen staining (% area) were quantified with ImageJ software.

Immunofluorescence (IF) staining

Liver tissue was embedded in Tissue-Tek OCT compound (Sakura Finetek, Sarku, Japan) and 4 μm thick sections were cut with a freezing microtome (Leica) at −20°C. The sections were incubated in 1% bovine serum albumin for 60 m to prevent nonspecific protein binding before they were labeled with a primary rabbit polyclonal F4/80 antibody (#ab100790; Abcam, Cambridge, UK) overnight at 4°C. The next day, they were washed with PBS and incubated with goat anti-rabbit IgG-CFL secondary antibody (#sc-362272; Santa Cruz Biotechnology) for 1 h at room temperature in the dark. The sections were viewed with a fluorescence microscope (Life Technologies, Carlsbad, CA, USA). The fluorescence intensity was measured in random fields of view using ImageJ software. We performed IF staining with anti-BAX (#60267-1-IG; Proteintech, Rosemont, IL, USA), DAPI (#G1012; Servicebio), CLEC4F antibody (#AF2784-SP; Novus Biologicals, Centennial, CO, USA), Albumin (#bs-2256R; Bioss, Woburn, MA, USA) and fluorescein (FITC) TdT-mediated dUTP-biotin nick end labeling (TUNEL) cell apoptosis detection kit (#GG1501; Servicebio).

Flow cytometry

Apoptosis of PMBCs and RAW 264.7 cells was assayed with a fluorescein isothiocyanate (FITC) Annexin V apoptosis detection kit I (#556547; BD Pharmingen, San Diego, CA, USA) according to the manufacturer's instructions. Briefly, after washing three times with fluorescence-activated cell sorting buffer, 1×10^6 cells per group were resuspended in 1×binding buffer (100 μL), and incubated with 5 μL Annexin V-FITC and 10 μL propidium iodide for 30 m at 4°C in the dark. The samples were assayed with a Coulter Epics XL flow cytometer (Beckman Coulter, Inc. Pasadena, CA, USA).

Ribonucleoprotein immunoprecipitation (RNP-IP)

RNP-IP has previously been used to show that ADAR1 binds to pre-miR-21 and pri-miR-30a in RAW 264.7 cells.[16,17] In this study, RNP-IP was performed to investigate whether ADAR1 bound to pre-miR-122. First, 2×10^7 RAW 264.7 cells were collected and lysed. The lysate was incubated with 30 mg anti-ADAR1 (#SC-73408; Santa Cruz Biotechnology) or anti-IgG antibodies (#2729; CST, Danvers, MA, USA) for 4 h at room temperature. Co-immunoprecipitated RNA was reverse transcribed and qRT-PCR was performed to determine the abundance of pre-miR-122 relative to U6.

Dual-luciferase reporter assay

A pmirGLO dual-luciferase miRNA target expression vector (GenePharma) containing wild-type (WT) or mutant (MUT) 3′-untranslated (UTR) region of BCL2A1 was constructed and cotransfected with the miR-122-5p mimic or mimic-NC into HEK 293T cells with Lipofectamine 3000 reagents (Inv-

itrogen). BCL2A1 homo 3′-UTR WT 5′-3′ UGUUGACCAGAAAGGACACUCCA; BCL2A1 homo 3′ UTR mutant 5′-3′ TGTTGTGGTGAAAGGTGTGAGGA, hsa-miR-122-5p mimic: 5′-3′ UGGAGUGUGACAAUGGUGUUUG, mimic-NC 5′-3′ UUCUCCGA ACGUGUCACGUTT. Twenty-four hours after transfection, the relative luciferase activity of the dual-luciferase reporter assay system was determined with an Infinite M1000 multimode microplate reader (Tecan, Männedorf, Switzerland) via dual-luciferase reporter assay system (Promega, Madison, WI, USA).

qRT-PCR

Total RNA was isolated from 50 mg of liver tissue using Trizol reagent kits (Invitrogen) according to the manufacturer's protocol. The same method was used to extract total RNA from RAW 264.7 cells and PBMCs of patients with sepsis. Specific primer pairs were designed by Tsingke Biotechnology (Beijing, China) and are listed in Supplementary Table 1. The primer pairs for miR-122-5p were synthesized by RiboBio (#miRA1001677-1-200).

Western blotting (WB)

Total protein was extracted using RIPA lysis buffer (GenStar, Beijing, China) with protease inhibitor cocktail (MedChemExpress, Shanghai, China). Protein concentration was determined with a bicinchoninic acid assay kit (Zhonghuihecai Biopharmaceutical Technology, Shaanxi, China). The primary antibodies used in our study were anti-Caspase3 cleaved (#19677-1-AP; Proteintech), anti-BAX (#60267-1-IG; Proteintech), anti-BCL2 (#AF6139; Affinity Biosciences, Cincinnati, OH, USA), anti-ADAR1 (#sc-73408; Santa Cruz), anti-BCL2A1a (#64310S; CST), and anti-β-actin (#3700; CST). β-actin was the internal reference.

Statistical analysis

SPSS Statistics 28.0 (IBM Corp., Armonk, NY, USA) was used for the statistical analysis and GraphPad Prism 9.0 (GraphPad, Inc., La Jolla, CA, USA) was used to generate graphs. Data were evaluated with the Shapiro–Wilk test to determine whether it was normally distributed. Student's *t*-tests were used to compare between-group differences of normally distributed results that were reported as means ± SDs). Mann–Whitney *U* tests were used to compare between-group differences of non-normally distributed results that were reported as medians and interquartile range (IQR). One-way analysis of variance with Tukey's multiple comparison test was used to compare differences among three or more groups. Log-rank Mantel–Cox) tests were used to compare between-group differences of survival curves. All animal and cell experiments were performed in at least three replicates. The threshold of statistical significance was $p<0.05$.

Results

Apoptosis of PBMCs significantly increases in patients with early sepsis

We collected PBMCs from healthy volunteers and patients with early sepsis, and observed the cellular morphology. Immune cells in the peripheral blood of healthy volunteers had normal morphology. PBMCs from patients with sepsis had degraded surface microvilli, shrunken cell membranes with local bulges, widened perinuclear spaces and pyknotic nuclei and mitochondria, all signs of apoptosis (Fig. 1A). Flow cytometry revealed that there was a significantly increased proportion of apoptotic and necrotic immune cells in patients with sepsis compared with healthy volunteers (Fig. 1B). In addition, in contrast to healthy volunteers, the plasma concentrations of inflammatory cytokines (IL-6 and TNF-α), chemokines (CCL4 and CXCL2), and pro-apoptotic indicators (BAX, TNFSF10, and NLRP3) increased significantly in patients with sepsis, especially those with severe sepsis, while the anti-apoptotic molecule (BCL2) showed a significant reduction in patients with sepsis (Fig. 1C and D). The clinical characteristics of patients with mild and severe sepsis patients are shown in Table 1. Blood immune cells and liver injury-related indicators were significantly higher in patients with severe sepsis than patients with mild sepsis, but patients with severe sepsis had significantly fewer monocytes.

Transcriptome sequencing of PBMCs revealed a total of 10,046 DEGs. Compared with healthy volunteers, there were 2,004 significantly upregulated DEGs and 3,698 significantly downregulated DEGs in patients with sepsis (Fig. 2A). KEGG and gene set enrichment analysis revealed that inflammatory response and apoptosis-related pathways were significantly enriched in patients with sepsis (Fig. 2B and C). A heatmap of DEGs revealed that ADAR1 and pro-apoptosis factors such as Toll-like receptors, tumor necrosis factor (TNF), BID, and caspase 4 (CASP4) were increased in patients with sepsis. However, unlike other members of the BCL2 family, the anti-apoptotic molecule BCL2A1 also increased significantly in patients with sepsis compared with healthy volunteers (Fig. 2D). The plasma concentrations of BID and BCL2A1 were also increased in patients with sepsis (Supplementary Fig. 1A).

Monocyte apoptosis is prominent in PBMCs from patients with early sepsis

We conducted single-cell sequencing of PBMCs from healthy volunteers and the sepsis groups to investigate DEGs in various immune cell subsets. We annotated five immune cells according to their cell markers, including monocytes, T and natural killer (NK) cells, neutrophils, B cells, and dendritic cells (DCs) (Fig. 3A). Among the cell types, monocytes had the largest number of DEGs in patients with sepsis (1,969 genes in total) compared with healthy volunteers (Fig. 3A); these genes were significantly enriched in apoptosis-related pathways (Fig. 3B and C). Similar to the transcriptome sequencing results, BCL2 family members were decreased in patients with sepsis, except for BCL2A1, which was significantly upregulated (Fig. 3D). The plasma concentration of the macrophage inflammatory-related proteins MIP3 and MIP3β was also significantly upregulated (Supplementary Fig. 1B). The results suggest that monocytes/macrophages had an important role in the pathological mechanism of immune cell death and immunosuppression in patients with sepsis.

Apoptosis of liver macrophages (Kupffer cells) is aggravated in a CLP-induced mouse model of sepsis

We used a mouse model of sepsis to explore sepsis-related apoptosis in different organs. After CLP, a large number of inflammatory cells infiltrated the lung and liver of septic mice, with significantly increased tissue injury scores and sepsis disease scores (Supplementary Fig. 2). TUNEL staining of lung and liver tissue showed that CLP-induced sepsis increased apoptosis much more prominently in the liver (Fig. 4A). We also evaluated relative protein and mRNA expression of apoptosis-related indicators in the liver of septic mice. The pro-apoptotic molecules caspase 3 and BAX were significantly increased, but the anti-apoptotic molecule BCL2 was significantly decreased after CLP (Fig. 4B and C). Double staining of liver tissue for TUNEL with ALB, F4/80, and CLEC4F revealed significantly higher apoptosis in Kuppfer (CLEC4F+)

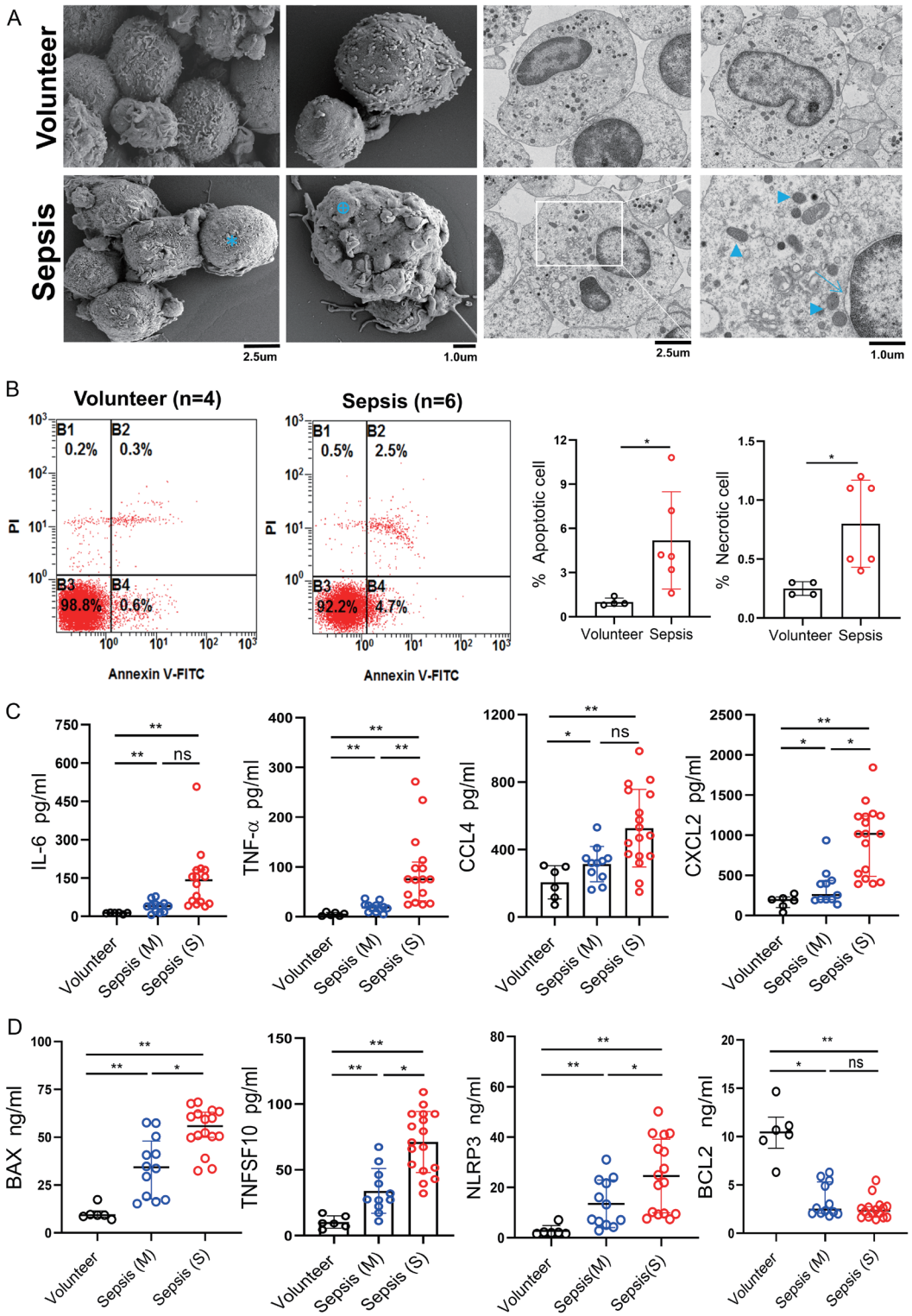

Fig. 1. Apoptosis of PBMCs was significantly increased in patients with sepsis. (A) SEM and TEM images of PBMCs from healthy volunteers and patients with sepsis. Asterisk (*) indicates degraded surface microvilli, cross (⊕) indicates local bulges, arrow (→) indicates widened perinuclear space, and triangle (▲) indicates pyknotic mitochondria. Scale bars mean 2.5 (left) and 1 (right) μm. (B) FCM analysis of the apoptosis proportion of PBMC cells in volunteers and patients with sepsis. Apoptotic cells were quantified in the B4 lower right quadrant (early apoptosis) and the B2 upper right (late apoptosis). Necrotic cells are seen in the B1 upper left quadrant. Volunteers n=4, Sepsis (M) n=6. (C) Plasma concentrations of inflammatory factors (IL6, TNF) and chemokines (CCL4, CXCL2) in volunteers and patients with sepsis. (D) Apoptotic molecules (BAX, TNFSF10, NLRP3, and BCL2) in the plasma of volunteers and patients with sepsis. Volunteers n=6, Sepsis (M) n=12, Sepsis (S) n=16. *p<0.05, **p<0.01. SEM, scanning electron microscopy; TEM, transmission electron microscopy.

Table 1. Clinical characteristics of sepsis patients

Parameter	Sepsis (M, *n*=12)	Sepsis (S, *n*=16)	χ^2/t/Z	*p*-value
Infection site				
Respiratory system, *n* (%)	5 (41.7)	7 (43.8)	0.21	1.00
Digestive system, *n* (%)	5 (41.7)	6 (37.5)		
Urogenital system, *n* (%)	2 (16.7)	3 (18.8)		
Physiological index				
Female, *n* (%)	5 (41.7)	6 (37.5)	NA	1.00
Age in years	68.67 ± 15.20	69.38 ± 13.43	0.13	0.897
Temperature in °C	37.78 ± 0.54	37.49 ± 0.72	1.20	0.242
Heart rate as r/m	108.75 ± 8.13	113.31 ± 11.79	1.15	0.261
Respiratory rate as r/m	24.00 ± 2.59	24.44 ± 2.28	0.47	0.640
MAP in mmHg	84.89 ± 3.39	60.92 ± 3.56	18.01	0.001**
Laboratory results				
WBC as $\times10^9$/L	11.65 ± 2.23	14.43 ± 2.80	2.83	0.009**
Neutrophil as $\times10^9$/L	9.69 ± 1.82	12.34± 2.76	2.89	0.008**
Lymphocyte as $\times10^9$/L	1.13 ± 0.46	1.39 ± 0.622	1.21	0.237
Monocyte as $\times10^9$/L	0.72 ± 0.32	0.48 ± 0.12	2.69	0.012*
PT in m	15.25 (13.03–16.55)	14.75 (14.23–15.85)	0.02	0.991
APTT in m	33.90 (31.65–37.83)	39.4 (34.48–43.13)	1.88	0.061
ALT in U/L	37.42 ± 8.15	89.38 ± 28.22	6.99	0.001**
AST in U/L	31.42 ± 6.78	114.50 ± 32.86	9.84	0.001**
Creatinine in μmol/L	102.42 ± 24.02	136.25 ± 51.79	2.30	0.031*
Lactic acid in mmol/L	1.10 ± 0.24	3.57 ± 0.87	10.88	0.001**
Disease score				
APACHE II	11.08 ± 1.62	17.63 ± 4.16	5.73	0.001**
SOFA	7.33 ± 1.61	10.88 ± 1.63	5.72	0.001**
Progress survival as %	11 (91.70)	10 (62.50)	NA	0.024*

The results are reported as numbers and percentage, means ± SD or medians and IQR. *p<0.05, **p<0.01. ALT, alanine aminotransferase; APACHE II, acute physiology and chronic health evaluation II; APTT, activated partial prothrombin time; AST, aspartate aminotransferase; MAP, mean arterial pressure; PT, prothrombin time; SBP, systolic blood pressure; SOFA, sequential organ failure assessment; WBC, white blood cell.

cells than in non-Kupffer cells in septic mice, 53.6 (IQR 46.0–61.7)% vs. 31.4 (IQR 24.9–35.8%) (p<0.01) (Fig. 4D).

ADAR1 reduces RAW 264.7 apoptosis after LPS treatment

To gain a deeper understanding of the effects of ADAR1 on macrophage apoptosis, we used RAW 264.7 cells, a murine macrophage cell line. Relative *Adar1* mRNA expression increased significantly 12 h after LPS treatment, and then decreased until 48 h (Fig. 5A). Because Adar1 expression is dynamic, we examined the effects 12 h after LPS treatment in subsequent experiments. The protein expression of BAX increased and BCL2A1a decreased in RAW 264.7 cells after ADAR1 knockdown (Fig. 5B), indicating a regulatory role of ADRA1 in macrophage apoptosis. We next overexpressed ADAR1 by infecting RAW 264.7 cells with ADAR1-overexpressing adenovirus (OE-ADAR1) and silenced ADARI by transfecting RAW 264.7 cells with ADAR1 siRNA. TEM showed that LPS promoted pronounced apoptotic morphology. Heterochromatin was aggregated at the nuclear margin, the perinuclear space was widened, and the mitochondria were shrunken with membranes having a high electron density. Flow cytometry revealed that the proportion of apoptotic RAW 264.7 cells increased significantly after LPS treatment. ADAR1 overexpression alleviated this change and ADAR1 inhibition aggravated it, leading to the appearance of pyknotic mitochondria, high matrix electron density, dilated cristae, and an increased proportion of apoptotic cells (Fig. 5C and D). Moreover, relative *Bax* and *Caspase3* mRNA expression increased after LPS administration. This increase was significantly reduced with ADAR1 overexpression and elevated with ADAR1 silencing. *Bcl2a1a* mRNA expression showed the opposite changes (Fig. 5E). BAX immunofluorescence staining was consistent with its mRNA expression in each study group (Supplementary Fig. 3A). Hence, the findings indicate that ADAR1 protected macrophages from apoptosis.

ADAR1 regulates macrophage apoptosis through the miR-122/BCL2A1 signaling pathway

ADAR1 regulates the biosynthesis of miRNAs through two mechanisms. In the nucleus, ADAR1 hinders miRNA biogenesis by A-to-I editing of pri-miRNAs.[25] In the cytoplasm,

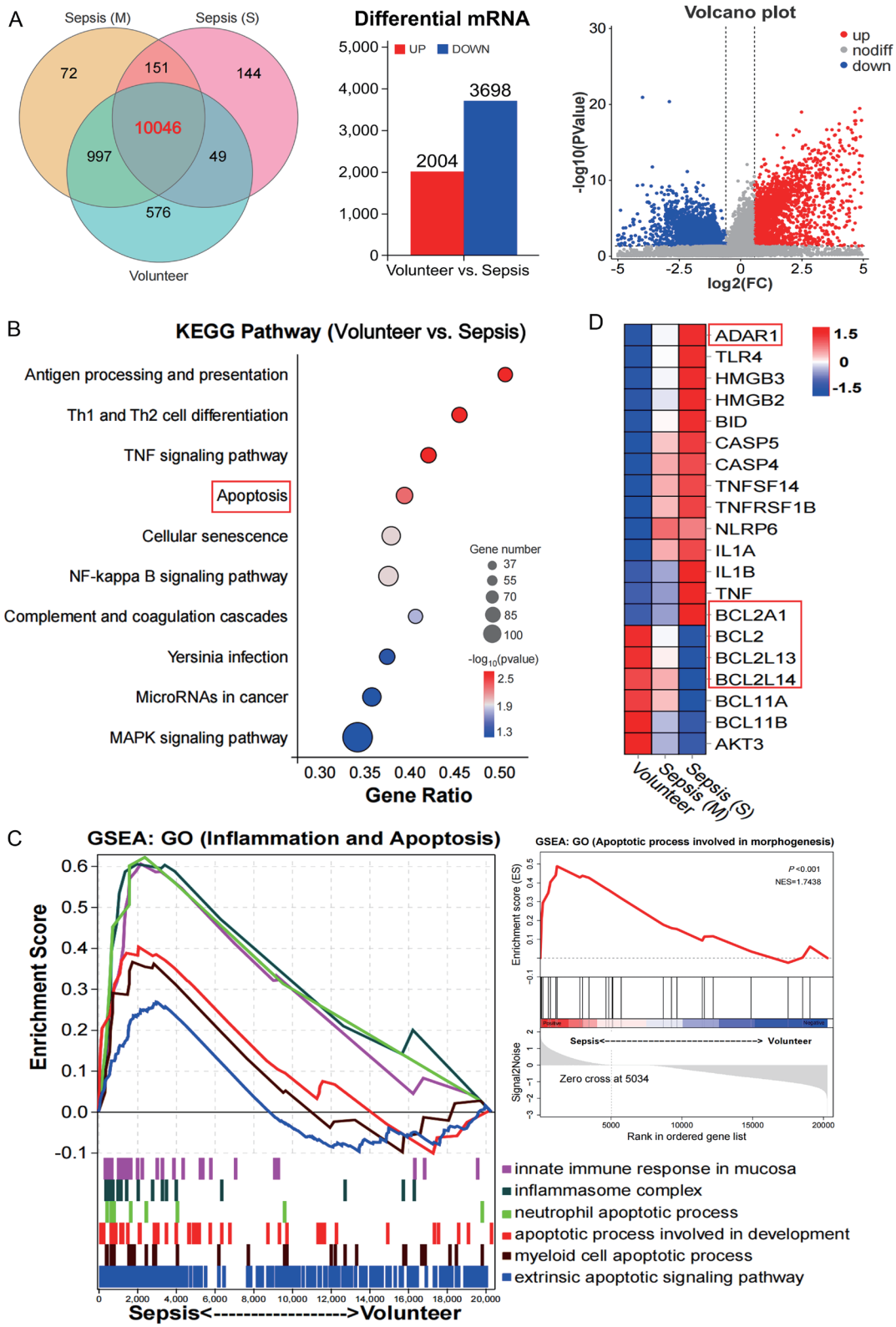

Fig. 2. mRNA sequencing of PBMCs from the patients with early sepsis. (A) Venn diagram, bar chart, and volcano map of the number and distribution of differential genes among groups. (B) KEGG functional analysis of the screened significant DEGs. (C) GSEA analysis of gene sets related to inflammatory and apoptosis pathways. (D) Heatmap showing the relative expression levels of the significant DEGs among groups. Volunteers n=7, Sepsis (M) n=5, Sepsis (S) n=4. All pathways are p<0.05. DEGs, differentially expressed genes; GO, gene ontology; GSEA, gene set enrichment analysis; KEGG, kyoto encyclopedia of genes and genomes.

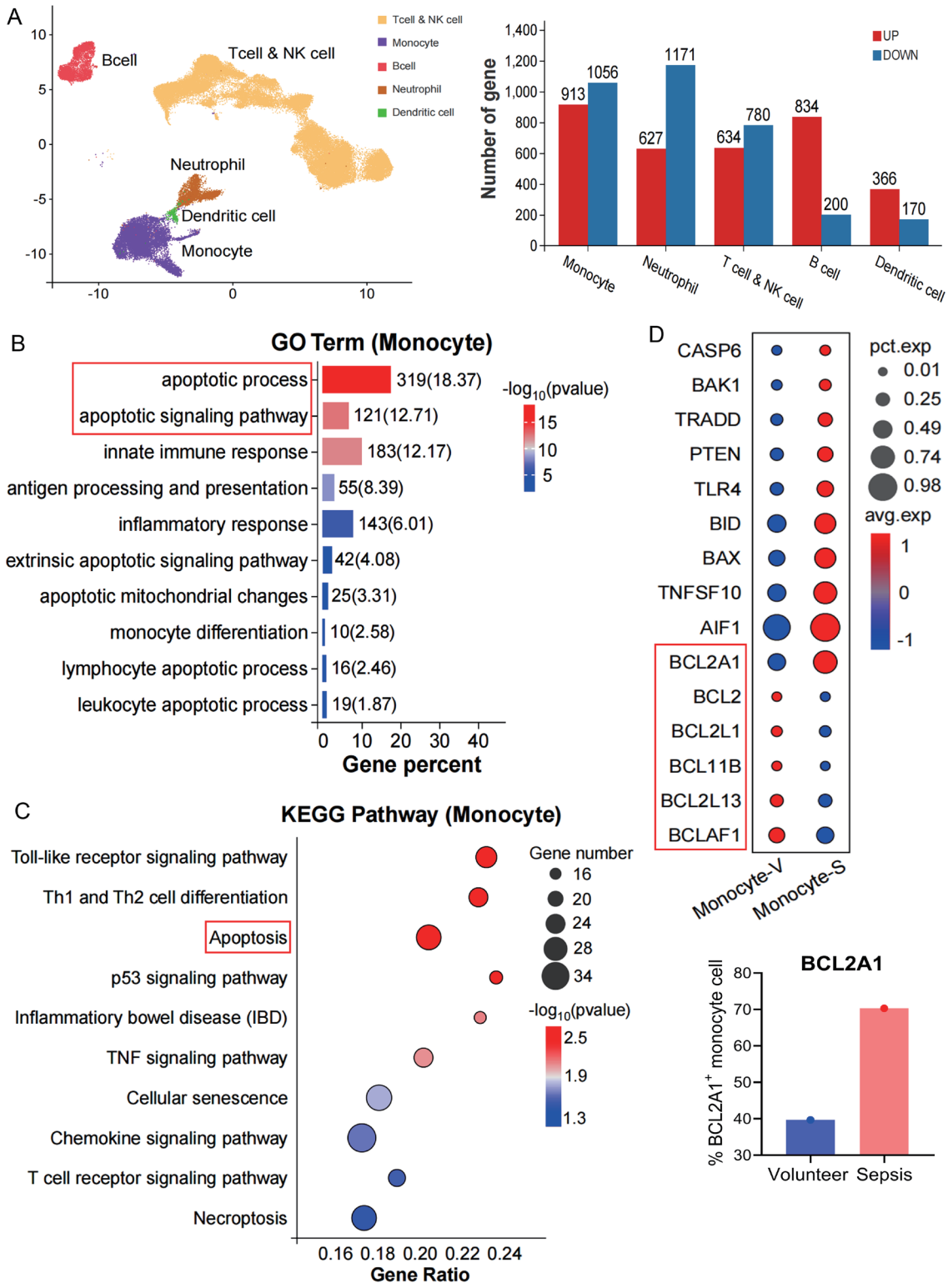

Fig. 3. Single cell RNA sequencing of PBMCs in volunteers and patients with sepsis. (A) After annotation with cell makers, PBMCs were divided into five groups of immune cells, among which monocytes had the largest number of DEGs. Monocytes: CD14/CD16/CD68/CD163/CSF1R/S100A12; Dendritic cells: CD11b/CD11c/CD15/CD83/CLEC4C/CD83/LYZ (lysozyme); Neutrophils: S100A8/S100A9; B cells: CD19/CD79a/CD79b/BLNK/MS4A1; T cell and NK cells: CD3d/CD3e/CD8a/CD27/CD28/NKG7/GZMB (granzyme B). (B, C) GO term and KEGG enrichment analysis of the DEGs in monocytes. (D) Bubble chart of the significant DEGs related to apoptosis. Volunteer n=3, Patients with sepsis n=3. The sepsis group included one mild case and two severe cases. The pathways were all p<0.05. DEGs, differentially expressed genes; GO, gene ontology; KEGG, kyoto encyclopedia of genes and genomes; NK cells, natural killer cells.

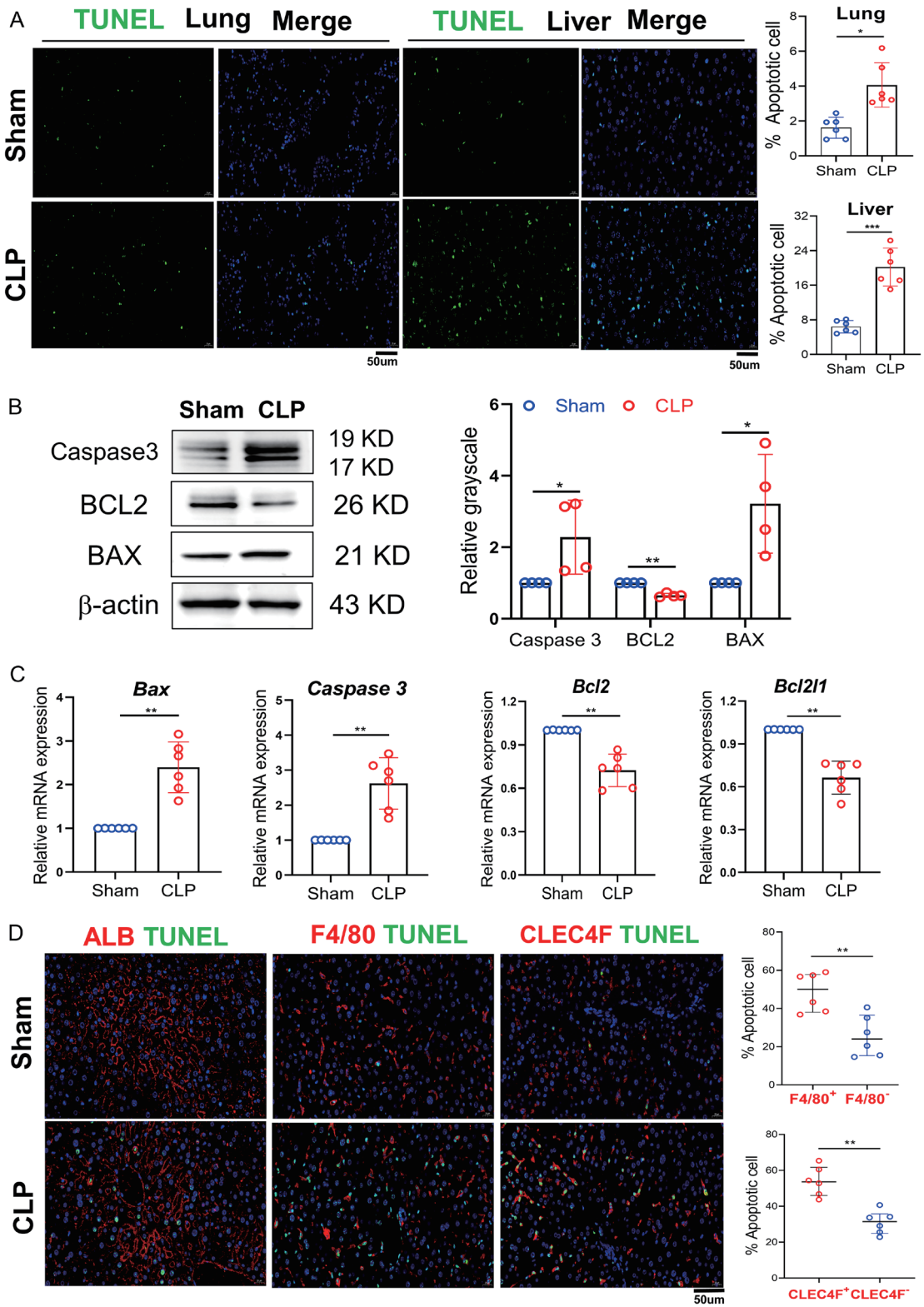

Fig. 4. Apoptosis of Kupffer cells was significantly increased in septic mice. (A) TUNEL staining of the lung and liver of CLP-induced septic mice. TUNEL-positive cells among the total number of cells in the analyzed field of view were quantified. Scale bars mean 50 μm. (B) Protein expression of apoptotic molecules Bax, Caspase3, and BCL2 in the livers of sham and septic mice. (C) Relative mRNA expression of apoptosis-related molecules in the livers of sham and septic mice (D) Immunofluorescence staining of TUNEL with ALB F4/80, and CLEC4F in the livers of the sham and septic mouse. TUNEL-positive cells of macrophages (F4/80+), Kupffer cells (CLEC4F+) and non-Kupffer cells (CLEC4F-) were quantified in septic mice. Scale bar=50 μm. *p<0.05, **p<0.01, ***p<0.001. CLP, cecal ligation and puncture.

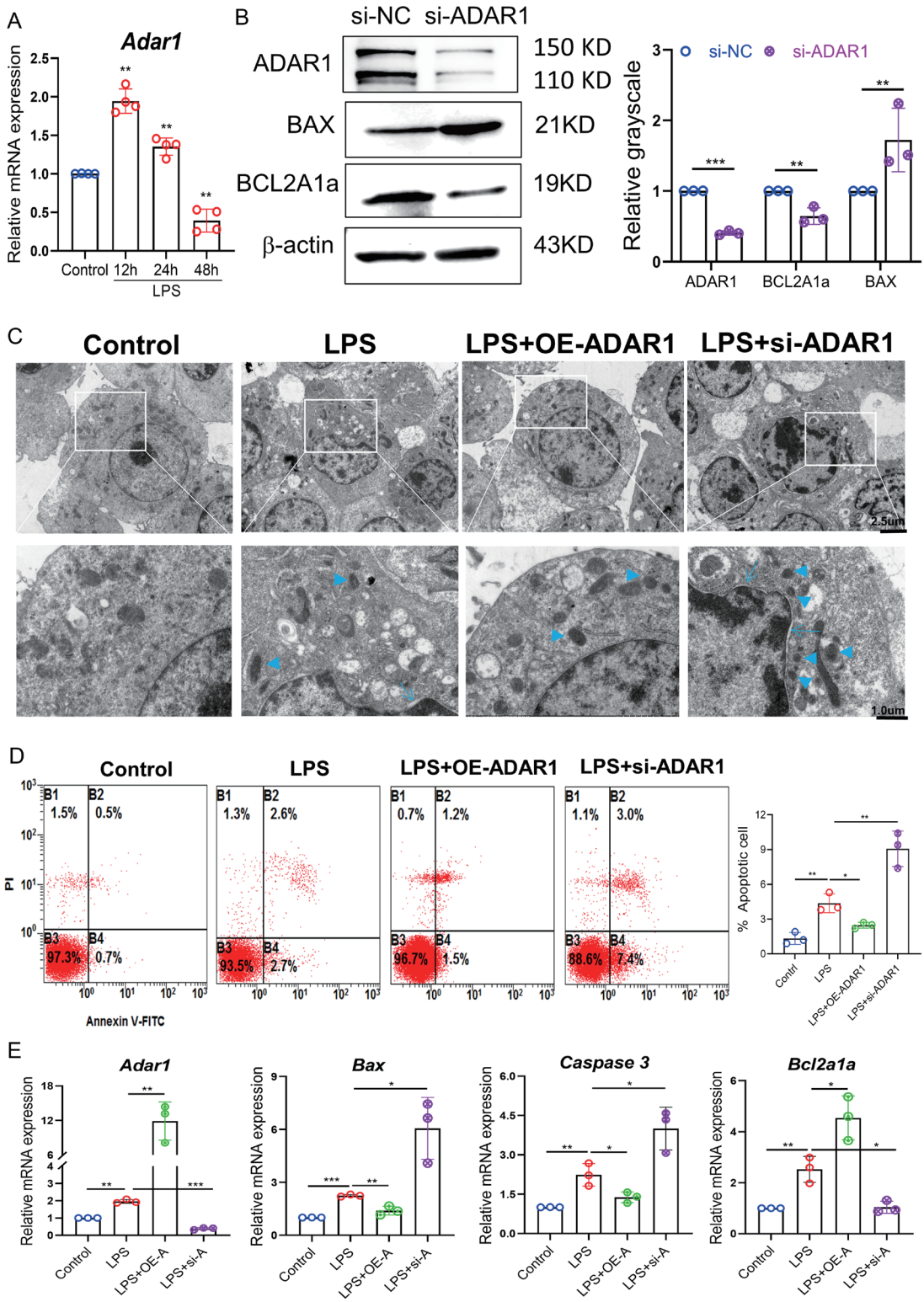

Fig. 5. ADAR1 reduced the apoptosis of RAW 264.7 cells that LPS treated. (A) *Adar1* expression in RAW 264.7 cells treated with LPS over time. (B) Western blot images and quantification of ADAR1, BAX, and BCL2A1a in RAW 264.7 cells transfected with si-ADAR1. (C) TEM images of RAW 264.7 cells transfected with OE-ADAR1 and si-ADAR1 12 h after LPS treated. Arrow (→) indicates widened perinuclear space and marginally gathered heterochromatin in the nucleus, and triangle (▲) indicates pyknotic mitochondria. Scale bars=2.5 (upper) and 1 (below) μm. (D) Flow cytometry analysis (Annexin V/PI staining) of RAW 264.7 cells transfected with OE-ADAR1 and si-ADAR1 after LPS treated. (E) *Bax, Caspase3*, and *Bcl2a1a* expressions in RAW 264.7 cells. *p<0.05, **p<0.01, ***p<0.001. LPS, lipopolysaccharide; OE-ADAR1, ADAR1-overexpressing adenovirus; si-ADAR1, ADRA1-small interfering RNA; si-NC, negative control-small interfering RNA; TEM, transmission electron microscopy.

ADAR1 forms a complex with Dicer to promote the generation of miRNA by enhancing Dicer cleavage activity.[13] We found significantly reduced *Dicer1* and *Ago2* mRNA expression in LPS-treated RAW264.7 cells (Supplementary Fig. 3B), suggesting that the synergism of ADAR1 and Dicer to promote miRNA production may be inhibited. In this case, a significant increase in ADAR1 may play a dominant role in its A-to-I editing effects.

We performed miRNA sequencing in PBMCs from healthy volunteers and patients with sepsis. There were 285 significantly upregulated miRNAs and 246 significantly downregulated miRNAs in patients with sepsis compared with healthy volunteers (Fig. 6A). KEGG and GO enrichment analysis indicated that differentially expressed miRNAs were significantly enriched in pathways related to apoptosis (Fig. 6B and Supplementary Fig. 4A). Among the top 10 significantly up- and downregulated miRNAs, miR-122, which is abundant in the liver, was significantly downregulated in patients with sepsis (Fig. 6C).[26] In addition, pri-miRNA-122 has been reported to contain high-frequency A-to-I editing sites (UAG triplet sequences) in its dsRNA regions.[27] Given that ADAR1 was significantly increased in patients with sepsis based on sequencing (Fig. 2D), we speculated that ADAR1 bound to miR-122 to hinder its biosynthesis through A-to-I editing. We predicted the potential interaction between ADAR1 and pre-miRNA-122 through RPISeq (http://pridb.gdcb.iastate.edu/RPISeq/). The support vector machine classifier value was 0.98, indicating a high possibility of interaction between ADAR1 and pre-miRNA-122. Moreover, the RNP-IP assay confirmed the direct binding effects of ADAR1 on pre-miR-122 (Fig. 6D). Meanwhile, qRT-PCR revealed that ADAR1 knockdown significantly upregulated miR-122-5p while ADAR1 overexpression markedly reduced miR-122-5p expression (Fig. 6E).

We also evaluated miR-122-5p expression in LPS-treated RAW 264.7 cells. MiR-122-5p decreased significantly 12 h after LPS administration, and then increased over time (Fig. 7A). After transfection with an miR-122 mimic, macrophage apoptosis increased (Fig. 7B and C). To determine how miR-122 modulated macrophage apoptosis, we predicted the target genes of miR-122-5p with Miranda (Version 3.3a), TargetScan (Version 7.0), and RNA hybrid (Version 2.1.2). A total of 3,237 target genes were predicted, including BCL2A1, which was significantly upregulated in patients with sepsis based on sequencing (Fig. 7D). A dual-luciferase assay confirmed the targeting effects of miR-122-5p on the 3′-UTR of BCL2A1 (Fig. 7E). Based on the NCBI database, we compared the targeted sequences of mmu-miR-122-5p and Bcl2a1a. Consistent with human genes, they also have paired binding sites and a targeting relationship (Supplementary Fig. 4B). Furthermore, *Bcl2a1a* mRNA levels in RAW 264.7 cells increased significantly 12 h after LPS treatment and then gradually, with significantly lower expression at 48 h compared with baseline (Fig. 7F). We transfected RAW 264.7 cells with the miR-122 mimic or inhibitor (we evaluated the transfection effects with qRT-PCR; Supplementary Fig. 4C), and determined the expression of Bcl2a1a with qRT-PCR and western blotting (Fig. 7G). The miR-122 mimic decreased BCL2A1a expression and the miR-122 inhibitor increased BCL2A1a expression. These results indicate that ADAR1 regulates macrophage apoptosis through the miR-122/BCL2A1 signaling axis.

The ADAR1/miR-122/BCL2A1 signaling pathway is involved in the regulation of Kupffer cell apoptosis in septic mice

We further verified the role of ADAR1 in macrophage apoptosis in the liver of septic mice. *Adar1* mRNA expression increased significantly 6 h after CLP and decreased significantly 24 and 48 h after CLP (Fig. 8A). We took 24 h as the modeling time for subsequent experiments. After infection with the ADAR1-overexpression adenovirus, CLP-induced septic mice had significantly disease scores and an elevated 7-day survival rate (Fig. 8B). Meanwhile, ADAR1 overexpression significantly increased BCL2A1a and decreased BAX mRNA and protein expression, and miR-122-5p expression was also reduced in the liver of septic mice (Figs. 8C, D, and Supplementary Fig. 5A). HE and immunofluorescence staining showed that ADAR1 overexpression significantly reduced the degree of pathological damage (Supplementary Figs. 5B and C) and the proportion of Kupffer cell apoptosis (CLEC4F+/TUNEL+) in septic livers (Fig. 8E and Supplementary Fig. 6). We also measured the plasma concentrations of inflammatory factors, liver injury markers, and apoptotic molecules. ADAR1 overexpression alleviated CLP-induced IL-6, ALT, and AST levels. Consistent with expectations, compared with the CLP group, ADAR1 overexpression significantly increased BCL2A1a expression and significantly decreased BAX expression (Fig. 8F). These findings collectively demonstrate that ADAR1 regulates liver monocyte/macrophage apoptosis under septic conditions by modulating the miR-122/BCL2A1 signaling pathway.

Discussion

Sepsis is a fatal systemic inflammatory disease caused by infection. The mortality rate of sepsis is approximately 25–30%, and 40–50% in patients with septic shock.[28,29] Postmortem studies have confirmed that immune cell apoptosis occurs in sepsis patients of all ages, and it is regarded as a major cause of the immunosuppressive pathophysiology of sepsis.[30] Our latest research has revealed the phenomenon of excessive monocyte apoptosis in the peripheral blood of patients with sepsis based on single-cell RNA sequencing.[31] Meanwhile, targeting apoptosis would be useful to reverse sepsis-induced immunosuppression, and manipulating apoptosis in sepsis is a novel therapeutic intervention in the clinic.[32,33] However, the issues of the underlying mechanism of immune cell apoptosis in sepsis and its induced organ injury are still not clear.

Immunosuppression in sepsis is manifested by reduced numbers and functional defects of immune cells. We found that monocytes in PBMCs had the most prominent pathological changes, further inducing the inflammatory response and organ damage. The apoptotic rate of liver Kupffer cells was also significantly increased in septic mice. Meanwhile, several pro-apoptotic molecules such as caspase-3 and BAX were significantly upregulated in murine RAW 264.7 macrophages treated with LPS. Under physiological conditions, there is a dynamic balance between cell apoptosis and proliferation. Under pathological conditions, this balance is broken.[34] Sustained apoptosis can lead to acute liver injury, such as fulminant hepatitis and reperfusion injury. Inhibition of excessive macrophage apoptosis is thus the key to alleviating acute liver injury.[34] Here, we comprehensively investigated the severity of monocyte/macrophage apoptosis in sepsis by evaluating clinical samples, an animal model, and an *in vitro* model.

Based on the sequencing results, the anti-apoptotic molecule BCL2A1, a member of the BCL2 family, was significantly increased in sepsis. We further confirmed that BCL2A1 was increased significantly in the LPS-treated RAW 264.7 cells, although it fell back in the later period. BCL2A1 is known to exert its anti-apoptotic functions by sequestering pro-apoptotic BCL2-family proteins (Bid and Bax). Downregulation of

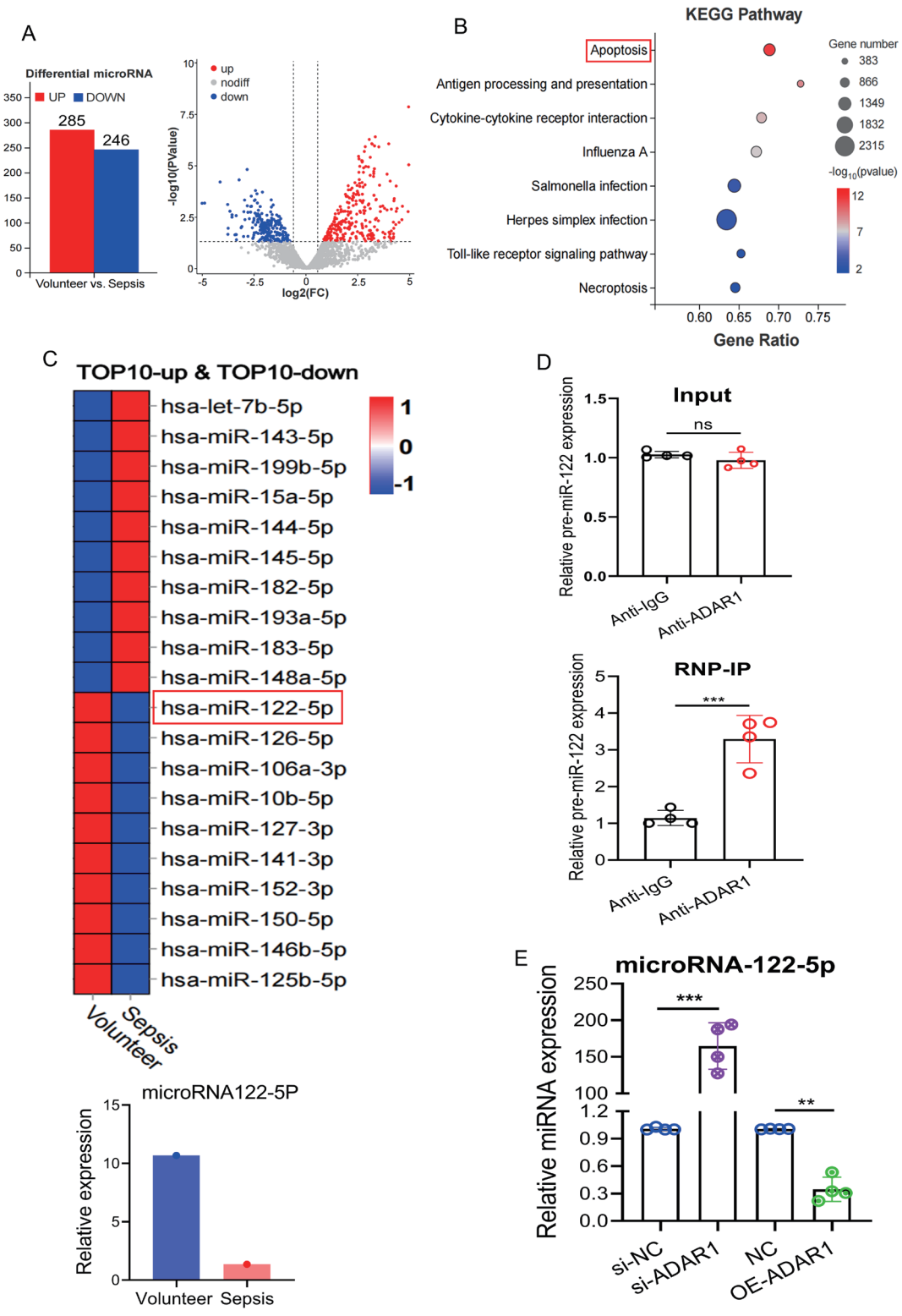

Fig. 6. miRNA sequencing of PBMCs from patients with early sepsis. (A) Bar chart and volcano plot of the number and distribution of differential miRNAs among groups. (B) KEGG pathway function analysis of the significant DE miRNAs. (C) Heatmap showing the top 10 significantly up- and downregulated differentially expressed miRNAs in the volunteer and sepsis groups. Volunteers n=5, patients with early sepsis n=8; (D) RNP-IP experiment confirmed the interaction between ADAR1 and miR-122. (E) Relative miR-122-5p expression in RAW 264.7 cells that were transfected with OE-ADAR1 and si-ADAR1. $^{**}p<0.01$, $^{***}p<0.001$. DE miRNAs, differentially expressed miRNAs; KEGG, kyoto encyclopedia of genes and genomes; OE-ADAR1, ADAR1-overexpressing adenovirus; RNP-IP, ribonucleoprotein immunoprecipitation; si-NC, negative control-small interfering RNA.

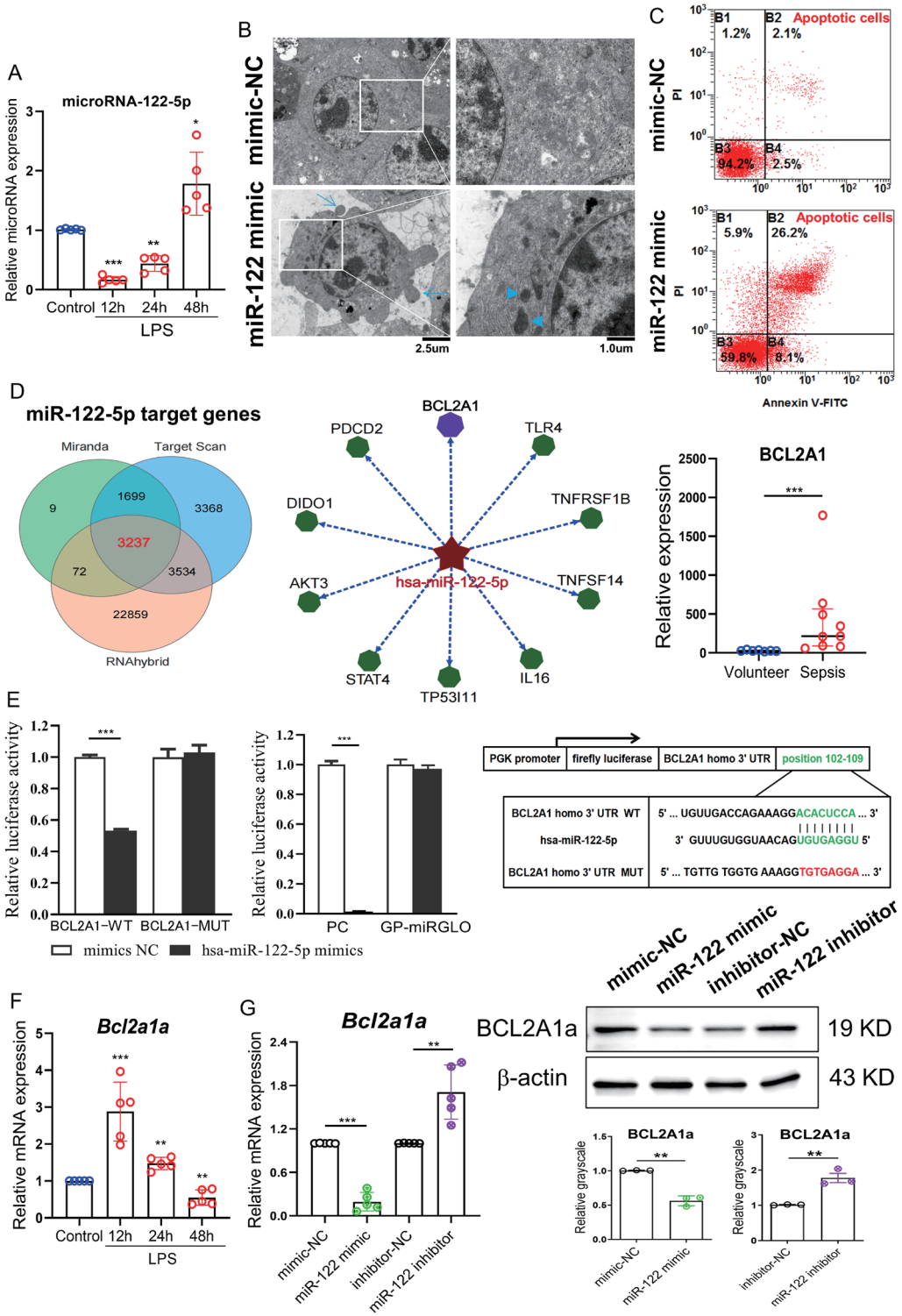

Fig. 7. MiR-122 regulated macrophages apoptosis by targeting BCL2A1. (A) Relative levels of miR-122-5p in RAW 264.7 cells that LPS treated over time. (B) TEM images of RAW 264.7 cells that were transfected with the miR-122 mimic 12 h after LPS treatment. Arrow (→) indicates the cell membrane sprouts and falls off, thus forming apoptotic bodies, and triangle (▲) indicates pyknotic mitochondria. Scale bars mean 2.5 (left) and 1 (right) μm. (C) FCM analysis of the percentage of apoptosis in RAW 264.7 cells that transfected with miR-122 mimic. (D) Potential target genes of miRNA122 were predicted using Miranda (Version 3.3a), TargetScan (Version 7.0), and RNA hybrid (Version 2.1.2), which included the anti-apoptotic molecule BCL2A1. The mRNA sequencing result of BCL2A1 is shown. (E) Dual-luciferase assay detected the binding of miR-122-5p on the 3′-UTR of BCL2A1 in RAW 264.7 cells. (F) *Bcl2a1a* expression in RAW 264.7 cells with LPS treated over time. (G) WB and qPCR assays evaluated the expression of BCL2A1a in RAW 264.7 cells that transfected with miR-122 mimic and inhibitor. **p*<0.05, ***p*<0.01, ****p*<0.001. LPS, lipopolysaccharide; MUT, mutant; NC, negative control; PC, positive control; WT, wild type; TEM, transmission electron microscopy.

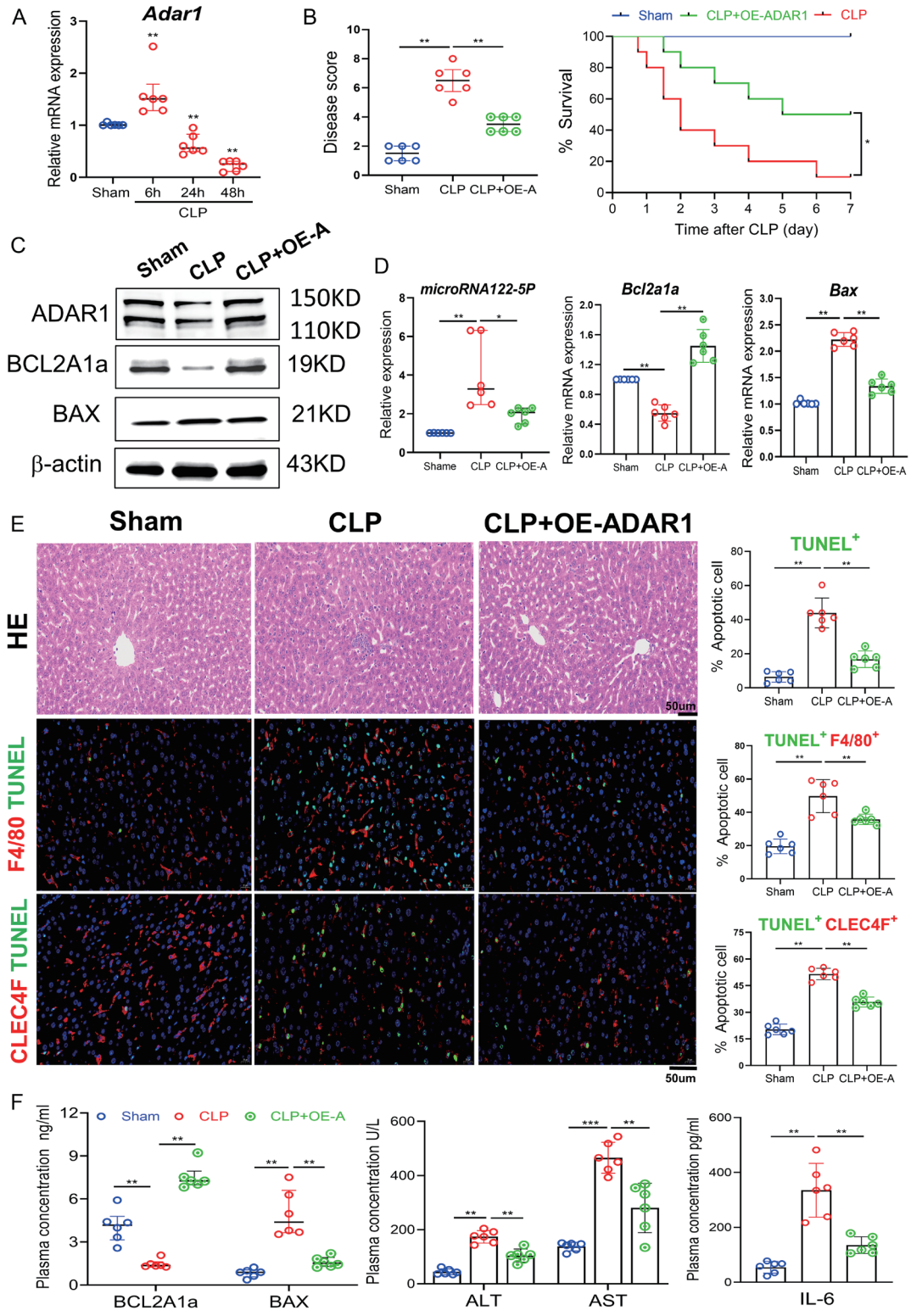

Fig. 8. ADAR1 reduced Kupffer cell apoptosis and alleviated sepsis-induced liver injury. (A) *Adar1* expression in the liver of CLP-induced septic mice over time. (B) After transfection with ADAR1 overexpression adenovirus, sepsis disease scores and 7-day survival rates of CLP-induced septic mice were evaluated (n=10). (C) Western blot images evaluated the protein levels of ADAR1, BCL2A1a, and BAX in the liver of sham, CLP, and CLP+OE-ADAR1 mice groups. (D) *miR-122-5p*, *Bcl2a1a*, and *Bax* expression in livers from the study groups. (E) HE and immunofluorescence (TUNEL with F4/80 and CLEC4F) staining of the liver in the study groups. (F) Concentration of apoptotic molecules (BCL2A1a and BAX), inflammatory factor (IL-6), and liver injury markers (ALT and AST) in the plasma of CLP model and CLP+OE-ADAR1 mice groups. *p<0.05, **p<0.01, ***p<0.001. CLP, cecal ligation and puncture; OE-ADAR1 (OE-A), ADAR1-overexpressing adenovirus.

BCL2A1 is associated with increased expression and translocation of cytochrome *c*, thus promoting cell apoptosis.[35] Other studies have revealed that BCL2A1 is significantly upregulated in patients with sepsis and is closely related to the prognosis of sepsis. Hence, it could represent a potential novel biomarker for the management of sepsis.[36] The question is what is the specific mechanism of BCL2A1-induced macrophage apoptosis in sepsis.

ADAR1 is expressed primarily in the brain, liver, lung, and kidney, and other tissues have little ADAR1 mRNA expression.[37,38] We found that with the progression of sepsis, ADAR1 expression increased initially and then decreased in the *in vivo* and *in vitro* experimental models. Meanwhile, ADAR1 expression differed with time and stimuli. Specifically, ADAR1 expression rose briefly and then decreased rapidly in a severe disease state (e.g., 1 μg/mL LPS treatment or CLP in which the free-end of cecum was ligated in the middle), but in milder disease (e.g., 200 ng/mL LPS treatment or CLP in which the free-end of cecum was ligated in the lower third), ADAR1 remain elevated for a prolonged period before falling. In RAW 64.7 cells, we analyzed changes in ADAR1 expression under moderate stimulation to simulate the acute phase of sepsis. Twelve hours of LPS treatment was more acceptable,[39,40] at which time ADAR1 expression in macrophages increased. We further verified the inhibitory effects of ADAR1 on macrophage apoptosis through animal experiments via a more severe CLP model. The disease was critical 24 h after CLP, which is often selected to evaluate organ injuries.[41,42] At this time, ADAR1 decreased in the liver and ADAR1 overexpression protected the liver from sepsis-induced injury.

ADAR1 regulates the biogenesis of miRNA precursors or mature miRNAs through its A-to-I editing activity, which has been well-accepted. We previously found that ADAR1 inhibited excessive inflammation in macrophages by editing miR-21 and miR-30a to further reduce organ damage.[16,17] Our sequencing results revealed that miR-122, a highly expressed liver-specific miRNA, was significantly reduced in PBMCs from patients with sepsis. Furthermore, interaction of ADAR1 with the miR-122 precursor was predicted and verified in this study. We found that ADAR1 negatively regulated miR-122 expression by binding to pre-miR-122 in macrophages.

Interestingly, a recent study reported a positive correlation between ADAR1 and miR-122 expression in hepatocytes.[43] We speculate that the expression of ADAR1 and miR-122 in various cell types likely determines their interaction. In hepatocytes, miR-122 is abundant. It makes up about 70% of the miRNA population in the adult liver.[44] A small amount of ADAR1 has limited editing effects on a very large number of miR-122 molecules. In this case, ADAR1 collaborating with Dicer may have a dominant role in promoting the generation of mature miR-122, resulting in a positive correlation between ADAR1 and miR-122. However, BioGPS data indicates that ADAR1 is abundantly expressed in macrophages and significantly increased in response to infection. Sufficient ADAR1 can fully edit pri-miR-122, and ultimately reduce the generation of miR-122. The role of ADAR1 in different cells may vary depending on its expression and that of miRNA. Additional study is required to clarify the detailed cellular mechanism. Furthermore, we predicted a targeting relationship between miR-122 and BCL2A1 based on the bioinformatics analysis and confirmed this relationship with a dual-luciferase assay and by assessing expression. After verification with animal experiments, we propose that the ADAR1/miR-122/BCL2A1 axis is involved in regulating liver macrophage (Kupffer cell) apoptosis in sepsis.

We also evaluated hepatocyte injury and found a higher proportion of hepatocyte apoptosis after CLP, which is consistent with previous studies.[45] In addition, ADAR1 overexpression significantly reduced the degree of pathological damage and the proportion of hepatocyte apoptosis, and the plasma concentrations of hepatocytes injury markers in septic livers. These findings collectively demonstrate that ADAR1 could be helpful to alleviate hepatocyte injury under septic conditions.

There are some study limitations. First, we collected patient samples from a single center and the sample size was small. Second, we used RAW 264.7 cells, a macrophage cell line, to only simulate sterile inflammation rather than true sepsis or infection. Third, the CLP-induced sepsis model results in polymicrobial infections in the abdominal cavity after intestinal injury, but does not simulate all subtypes, such as sepsis-induced liver injury caused by the spread of pathogenic bacteria from distant infection sites. Hence, additional large multicenter studies with different of sepsis subtypes are needed.

In conclusion, we showed that ADAR1 protected against sepsis-induced liver injury. ADAR1 overexpression significantly alleviated CLP-induced liver injury and reduced Kupffer cell/macrophage apoptosis through the miR-122/BCL2A1 signaling pathway. The ADAR1/miR-122/BCL2A1 axis may represent a target for the treatment of sepsis-related liver injury. This eventuality should be assessed with additional clinical studies to confirm the regulatory roles in sepsis.

Acknowledgments

The authors thank the volunteers for their time and dedication to participate in our study. In addition, the authors thank medical statistical expert Professor Yuhai Zhang from the Department of Statistics, the Fourth Military Medical University for his assistance in carefully reviewing the statistical analysis described the manuscript.

Funding

This work was supported by the Basic research program of Natural Science in Shaanxi Province (No. 2020JQ-466), Key research and development program of Shaanxi Province (No. 2021SF-014), University Supporting Grant (No. 2020rcfczr), Basic research project of the Logistics Support Department of the Chinese Military Commission (No. BWS21J002), and National Natural Science Foundation of China (No. 81871587).

Conflict of interest

The authors have no conflict of interests related to this publication.

Author contributions

Conceived of the study and participated in its design and coordination (WY, RZ, JL), designed and conducted the experiments (SL, JX, XZ, MY), collected peripheral blood samples and performed the statistical analysis (ZF, ZD, XL, YL), drafted the manuscript (SL, CD), and helped revise the manuscript (WY, RZ). All authors made significant contributions to this study and have approved the final manuscript.

Ethical statement

The study was approved by the Ethical Committee of the Xijing Hospital of Fourth Military Medical University, with document numbers of KY20212172 and NCT05229328. All procedures involving human participants complied with the

Declaration of Helsinki. Informed consent was signed by all healthy volunteers and patients with sepsis. Animal experiments were carried out according to the Guide for the Care and Use of Laboratory Animals and approved by the Institutional Animal Care and Use Committee of the Fourth Military Medical University (approved number: 20220930).

Data sharing statement

The data presented in the study are deposited in the NCBI Sequence Read Archive database, accession number PRJNA954715 (mRNA sequencing) and PRJNA954731 (miRNA sequencing). Other data that support the findings of this study are available from the corresponding author upon reasonable request.

References

[1] Singer M, Deutschman CS, Seymour CW, Shankar-Hari M, Annane D, Bauer M, *et al*. The Third International Consensus Definitions for Sepsis and Septic Shock (Sepsis-3). JAMA 2016;315(8):801–810. doi:10.1001/jama.2016.0287, PMID:26903338.

[2] Rudd KE, Johnson SC, Agesa KM, Shackelford KA, Tsoi D, Kievlan DR, *et al*. Global, regional, and national sepsis incidence and mortality, 1990-2017: analysis for the Global Burden of Disease Study. Lancet (London, England) 2020;395(10219):200–211. doi:10.1016/S0140-6736(19)32989-7, PMID:31954465.

[3] Lelubre C, Vincent JL. Mechanisms and treatment of organ failure in sepsis. Nat Rev Nephrol 2018;14(7):417–427. doi:10.1038/s41581-018-0005-7, PMID:29691495.

[4] Kalal CR, Joshi H, Kumar V, Gopal D, Rathod D, Shukla A, *et al*. Clinical Significance of Liver Function Abnormality in Patients with COVID-19: A Single-center Experience from Western India. J Clin Transl Hepatol 2021;9(6):878–888. doi:10.14218/JCTH.2020.00099, PMID:34966651.

[5] Yan J, Li S, Li S. The role of the liver in sepsis. Int Rev Immunol 2014;33(6):498–510. doi:10.3109/08830185.2014.889129, PMID:24611785.

[6] Huang M, Cai S, Su J. The Pathogenesis of Sepsis and Potential Therapeutic Targets. Int J Mol Sci 2019;20(21):5376. doi:10.3390/ijms20215376, PMID:31671729.

[7] van der Poll T, Opal SM. Host-pathogen interactions in sepsis. Lancet Infect Dis 2008;8(1):32–43. doi:10.1016/S1473-3099(07)70265-7, PMID:18063412.

[8] Li M, Song K, Huang X, Fu S, Zeng Q. GDF-15 prevents LPS and D-galactosamine-induced in flammation and acute liver injury in mice. Int J Mol Med 2018;42(3):1756–1764. doi:10.3892/ijmm.2018.3747, PMID:29956733.

[9] Savio LEB, de Andrade Mello P, Figliuolo VR, de Avelar Almeida TF, Santana PT, Oliveira SDS, *et al*. CD39 limits P2X7 receptor inflammatory signaling and attenuates sepsis-induced liver injury. J Hepatol 2017;67(4):716–726. doi:10.1016/j.jhep.2017.05.021, PMID:28554875.

[10] Liang X, Li T, Zhou Q, Pi S, Li Y, Chen X, *et al*. Mesenchymal stem cells attenuate sepsis-induced liver injury via inhibiting M1 polarization of Kupffer cells. Mol Cell Biochem 2019;452(1-2):187–197. doi:10.1007/s11010-018-3424-7, PMID:30178273.

[11] Otto GP, Sossdorf M, Claus RA, Rodel J, Menge K, Reinhart K, *et al*. The late phase of sepsis is characterized by an increased microbiological burden and death rate. Crit Care 2011;15(4):R183. doi:10.1186/cc10332, PMID:21798063.

[12] Peck-Palmer OM, Unsinger J, Chang KC, McDonough JS, Perlman H, McDunn JE, *et al*. Modulation of the Bcl-2 family blocks sepsis-induced depletion of dendritic cells and macrophages. Shock 2009;31(4):359–366. doi:10.1097/SHK.0b013e31818ba2a2, PMID:18838943.

[13] Ota H, Sakurai M, Gupta R, Valente L, Wulff BE, Ariyoshi K, *et al*. ADAR1 forms a complex with Dicer to promote microRNA processing and RNA-induced gene silencing. Cell 2013;153(3):575–589. doi:10.1016/j.cell.2013.03.024, PMID:23622242.

[14] Chung H, Calis JJA, Wu X, Sun T, Yu Y, Sarbanes SL, *et al*. Human ADAR1 Prevents Endogenous RNA from Triggering Translational Shutdown. Cell 2018;172(4):811–824.e814. doi:10.1016/j.cell.2017.12.038, PMID:29395325.

[15] Liu S, Xie J, Zhao B, Hu X, Li X, Zhang B, *et al*. ADAR1 prevents small intestinal injury from inflammation in a murine model of sepsis. Cytokine 2018;104:30–37. doi:10.1016/j.cyto.2018.01.020, PMID:29414324.

[16] Shangxun Z, Junjie L, Wei Z, Yutong W, Wenyuan J, Shanshou L, *et al*. ADAR1 Alleviates Inflammation in a Murine Sepsis Model via the ADAR1-miR-30a-SOCS3 Axis. Mediators Inflamm 2020;2020:9607535. doi:10.1155/2020/9607535, PMID:32273831.

[17] Li J, Xie J, Liu S, Li X, Zhang D, Wang X, *et al*. ADAR1 attenuates allogeneic graft rejection by suppressing miR-21 biogenesis in macrophages and promoting M2 polarization. FASEB J 2018;32(9):5162–5173. doi:10.1096/fj.201701449R, PMID:29694248.

[18] Evans L, Rhodes A, Alhazzani W, Antonelli M, Coopersmith CM, French C, *et al*. Surviving sepsis campaign: international guidelines for management of sepsis and septic shock 2021. Intensive Care Med 2021;47(11):1181–1247. doi:10.1007/s00134-021-06506-y, PMID:34599691.

[19] Rittirsch D, Huber-Lang MS, Flierl MA, Ward PA. Immunodesign of experimental sepsis by cecal ligation and puncture. Nat Protoc 2009;4(1):31–36. doi:10.1038/nprot.2008.214, PMID:19131954.

[20] Weber GF, Chousterman BG, He S, Fenn AM, Nairz M, Anzai A, *et al*. Interleukin-3 amplifies acute inflammation and is a potential therapeutic target in sepsis. Science 2015;347(6227):1260–1265. doi:10.1126/science.aaa4268, PMID:25766237.

[21] Park CY, Heo JN, Suk K, Lee WH. Sodium azide suppresses LPS-induced expression MCP-1 through regulating IkappaBzeta and STAT1 activities in macrophages. Cell Immunol 2017;315:64–70. doi:10.1016/j.cellimm.2017.02.007, PMID:28391993.

[22] Ishak K, Baptista A, Bianchi L, Callea F, De Groote J, Gudat F, *et al*. Histological grading and staging of chronic hepatitis. J Hepatol 1995;22(6):696–699. doi:10.1016/0168-8278(95)80226-6, PMID:7560864.

[23] Saffioti F, Hall A, de Krijger M, Verheij J, Hubscher SG, Maurice J, *et al*. Collagen proportionate area correlates with histological stage and predicts clinical events in primary sclerosing cholangitis. Liver Int 2021;41(11):2681–2692. doi:10.1111/liv.14979, PMID:34051052.

[24] He H, Liu L, Chen Q, Liu A, Cai S, Yang Y, *et al*. Mesenchymal Stem Cells Overexpressing Angiotensin-Converting Enzyme 2 Rescue Lipopolysaccharide-Induced Lung Injury. Cell Transplant 2015;24(9):1699–1715. doi:10.3727/096368914X685087, PMID:25291359.

[25] Nishikura K. Functions and regulation of RNA editing by ADAR deaminases. Annu Rev Biochem 2010;79:321–349. doi:10.1146/annurev-biochem-060208-105251, PMID:20192758.

[26] Jopling C. Liver-specific microRNA-122: Biogenesis and function. RNA Biol 2012;9(2):137–142. doi:10.4161/rna.18827, PMID:22258222.

[27] Kawahara Y, Megraw M, Kreider E, Iizasa H, Valente L, Hatzigeorgiou AG, *et al*. Frequency and fate of microRNA editing in human brain. Nucleic Acids Res 2008;36(16):5270–5280. doi:10.1093/nar/gkn479, PMID:18684997.

[28] Walkey AJ, Lagu T, Lindenauer PK. Trends in sepsis and infection sources in the United States. A population-based study. Ann Am Thorac Soc 2015;12(2):216–220. doi:10.1513/AnnalsATS.201411-498BC, PMID:25569845.

[29] Cecconi M, Evans L, Levy M, Rhodes A. Sepsis and septic shock. Lancet 2018;392(10141):75–87. doi:10.1016/S0140-6736(18)30696-2, PMID:29937192.

[30] Zheng X, Chen W, Gong F, Chen Y, Chen E. The Role and Mechanism of Pyroptosis and Potential Therapeutic Targets in Sepsis: A Review. Front Immunol 2021;12:711939. doi:10.3389/fimmu.2021.711939, PMID:34305952.

[31] Liu S, Duan C, Xie J, Zhang J, Luo X, Wang Q, *et al*. Peripheral immune cell death in sepsis based on bulk RNA and single-cell RNA sequencing. Heliyon 2023;9(7):e17764. doi:10.1016/j.heliyon.2023.e17764, PMID:37455967.

[32] Cao C, Yu M, Chai Y. Pathological alteration and therapeutic implications of sepsis-induced immune cell apoptosis. Cell Death Dis 2019;10(10):782. doi:10.1038/s41419-019-2015-1, PMID:31611560.

[33] Le Tulzo Y, Pangault C, Gacouin A, Guilloux V, Tribut O, Amiot L, *et al*. Early circulating lymphocyte apoptosis in human septic shock is associated with poor outcome. Shock 2002;18(6):487–494. doi:10.1097/00024382-200212000-00001, PMID:12462554.

[34] Tian LL, Zhang J, Wang ZZ, Chen SC, Zou XB, Yu ZK, *et al*. KLF15 reduces the level of apoptosis in mouse liver induced by sepsis by inhibiting p38MAPK/ERK1/2 signaling pathway. Eur Rev Med Pharmacol Sci 2020;24(20):10819–10828. doi:10.26355/eurrev_202010_23444, PMID:33155243.

[35] Zheng Q, Gan G, Gao X, Luo Q, Chen F. Targeting the IDO-BCL2A1-Cytochrome c Pathway Promotes Apoptosis in Oral Squamous Cell Carcinoma. Onco Targets Ther 2021;14:1673–1687. doi:10.2147/OTT.S288692, PMID:33707952.

[36] Li J, Zhou M, Feng JQ, Hong SM, Yang SY, Zhi LX, *et al*. Bulk RNA Sequencing With Integrated Single-Cell RNA Sequencing Identifies BCL2A1 as a Potential Diagnostic and Prognostic Biomarker for Sepsis. Front Public Health 2022;10:937303. doi:10.3389/fpubh.2022.937303, PMID:35832273.

[37] Mohamad MI, Desoky IA, Ahmed Zaki K, Sadek DR, Kamal Kassim S, Abdel-Wahab Mohamed D. Pterostilbene ameliorates the disrupted Adars expression and improves liver fibrosis in DEN-induced liver injury in Wistar rats: A novel potential effect. Gene 2022;813:146124. doi:10.1016/j.gene.2021.146124, PMID:34921950.

[38] Omata Y, Okawa M, Haraguchi M, Tsuruta A, Matsunaga N, Koyanagi S, *et al*. RNA editing enzyme ADAR1 controls miR-381-3p-mediated expression of multidrug resistance protein MRP4 via regulation of circRNA in human renal cells. J Biol Chem 2022;298(8):102184. doi:10.1016/j.jbc.2022.102184, PMID:35753353.

[39] Yang LY, Shen SC, Cheng KT, Subbaraju GV, Chien CC, Chen YC. Hispolon inhibition of inflammatory apoptosis through reduction of iNOS/NO production via HO-1 induction in macrophages. J Ethnopharmacol 2014;156:61–72. doi:10.1016/j.jep.2014.07.054, PMID:25128739.

[40] Zhang H, Guo C, Zhang A, Fan Y, Gu T, Wu D, *et al*. Effect of S-aspirin, a novel hydrogen-sulfide-releasing aspirin (ACS14), on atherosclerosis in apoE-deficient mice. Eur J Pharmacol 2012;697(1-3):106–116. doi:10.1016/j.ejphar.2012.10.005, PMID:23085268.

[41] Tajima G, Tokunaga A, Umehara T, Ikematsu K, Miyamoto J, Sato S, *et al*. Early diagnosis using established discriminant analysis of innate immune receptor gene expression profiles in a murine infectious or sterile systemic inflammation model. J Trauma Acute Care Surg 2018;84(4):583–589. doi:10.1097/TA.0000000000001789, PMID:29287057.

[42] Coldewey SM, Rogazzo M, Collino M, Patel NS, Thiemermann C. Inhibition of IkappaB kinase reduces the multiple organ dysfunction caused by sepsis in the mouse. Dis Model Mech 2013;6(4):1031–1042. doi:10.1242/dmm.012435, PMID:23649820.

[43] Liu G, Ma X, Wang Z, Wakae K, Yuan Y, He Z, *et al*. Adenosine deaminase acting on RNA-1 (ADAR1) inhibits hepatitis B virus (HBV) replication by enhancing microRNA-122 processing. J Biol Chem 2019;294(38):14043–14054. doi:10.1074/jbc.RA119.007970, PMID:31366735.
[44] Hassan M, Elzallat M, Aboushousha T, Elhusseny Y, El-Ahwany E. MicroRNA-122 mimic/microRNA-221 inhibitor combination as a novel therapeutic tool against hepatocellular carcinoma. Noncoding RNA Res 2023;8(1):126–134. doi:10.1016/j.ncrna.2022.11.005, PMID:36474748.
[45] Yang Q, Yang Y, Shi Y, Lv F, He J, Chen Z. Effects of Granulocyte Colony-Stimulating Factor on Patients with Liver Failure: a Meta-Analysis. J Clin Transl Hepatol 2016;4(2):90–96. doi:10.14218/JCTH.2016.00012, PMID:27350939.